

# Electrical Properties of Metal-Diamond-Like-Nanocomposite (Me-DLN) Contacts to 6H SiC

K.J. SCHOEN,\* J.M. WOODALL,\* A. GOEL,† and C. VENKATRAMAN†

\*School of Electrical and Computer Engineering and the Engineering Research Center for Collaborative Manufacturing, Purdue University, West Lafayette, IN 47907

†Advanced Refractory Technologies Inc., Buffalo, NY 14207

We have fabricated tungsten-diamond-like-nanocomposite (W-DLN) Schottky contacts on n-type and p-type 6H SiC (Si-face). The as-deposited n-type and p-type contacts are rectifying and measurement results suggest that the electrical characteristics are dominated by the properties of the tungsten SiC interface. The n-type contacts have a reverse leakage current density of  $4.1 \times 10^{-3} \text{ Acm}^{-2}$  and the p-type contacts have a reverse leakage current density of  $1.4 \times 10^{-7} \text{ Acm}^{-2}$  at  $-10 \text{ V}$ . The n-type contacts have a current-voltage (I-V) extracted effective  $\phi_{Bn}$  of 0.7 eV with an ideality factor of 1.2 and a capacitance-voltage (C-V) extracted  $\phi_{Bn}$  of 1.2 eV. The p-type contacts have an I-V extracted effective  $\phi_{Bp}$  of 1.8 eV with an ideality factor of 1.7. Non-ideal I-V and C-V characteristics may be due to surface damage during W-DLN deposition.

**Key words:** High temperature contacts, metal-diamond-like-nanocomposite, Schottky barrier contacts, silicon carbide, tungsten

## INTRODUCTION

Large bandgap semiconductors have been widely investigated for use in optoelectronic applications. However, research interest in large bandgap and SiC electrical devices has recently increased due to the commercial availability of high quality SiC and general advances in large bandgap material fabrication techniques. SiC is a promising high temperature and high voltage semiconductor because of its large bandgap (2.2 eV for 3C, 3.0 eV for 6H, and 3.2 eV for 4H) and its thermal stability. For power applications, SiC's large bandgap translates into a high critical electric field. A high critical electric field allows device designs which have lower series resistance and lower power dissipation for a given breakdown voltage. For high temperature applications, SiC's large bandgap results in fewer intrinsic carriers at a given temperature. This enables devices to operate at high temperatures because the intrinsic carrier concen-

tration remains low relative to the impurity doping concentration. The critical electric field and the intrinsic carrier concentration (at 27°C) for silicon, GaAs, and 4H SiC are given in Table I.

High voltage and high temperature electronics offer the potential for substantial cost savings by improving existing electronic systems and by the advancement of electronic systems into new areas of application. Since high voltage devices may experience significant self-heating, the development of reliable, thermally stable device structures will benefit both high voltage and high temperature applications.

Basic SiC processing technology has been rapidly evolving through advances in oxide growth, ion implantation doping, mesa etching, and contact formation. These advances have allowed the development and demonstration of relatively complex integrated circuits (NVRAMs,<sup>1</sup> CCDs,<sup>2</sup> and complementary metal oxide semiconductor [CMOS] logic<sup>3</sup>) and high performance discrete power devices (IGBTs,<sup>4</sup> SITs,<sup>5</sup> metal-oxide semiconductor field effect transistors [MOSFETs],<sup>6,7</sup> PN diodes,<sup>8</sup> and Schottky diodes).<sup>9</sup>

**Table I. Critical Electric Field and Intrinsic Carrier Concentration for Silicon, GaAs, and 4H SiC**

Material	$E_{CR}$ V/cm	$n_i$ at 27°C $cm^{-3}$
Si	$3 \times 10^5$	$1.45 \times 10^{10}$
GaAs	$4 \times 10^5$	$1.79 \times 10^6$
4H SiC	$2.4 \times 10^6$	$1.6 \times 10^{-8}$

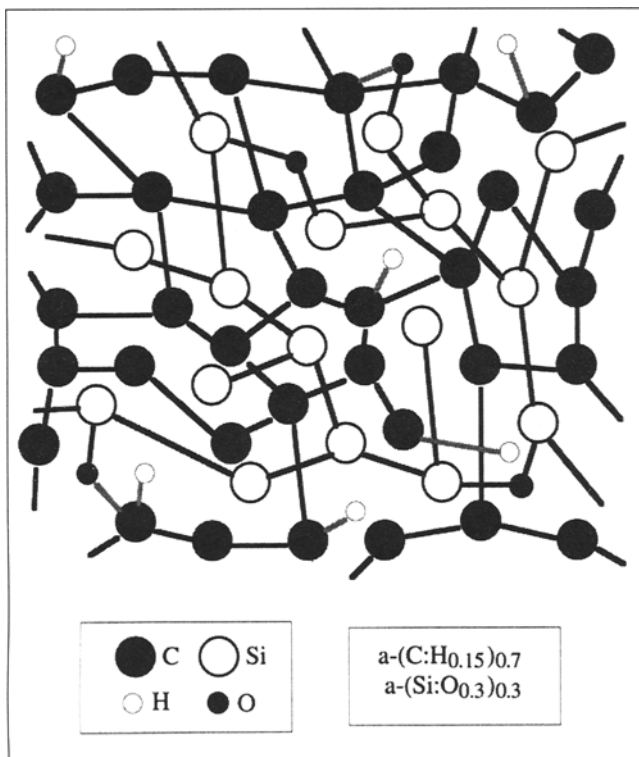


Fig. 1. Basic structure of diamond-like-nanocomposite. Structure contains carbon networks terminated by hydrogen and silicon networks terminated by oxygen. Carbon to carbon bonds are predominately  $sp^3$  or diamond-like bonds.

However, new contact technologies have not been developed which fully leverage the high voltage and high temperature capabilities of SiC. The high temperature performance of some device structures has been limited by the lack of a high temperature contact technology. High temperature JFETs have been reported to operate for 30 h at 600°C in air with the only reported degradation being due to the oxidation of the metals used for electrical contacts.<sup>10</sup> Thus, high temperature contacts are a critical technology impeding further device and system development.

### DIAMOND-LIKE-NANOCOMPOSITE AND METAL-DLN

Metal-diamond-like nanocomposite (Me-DLN) is a potentially interesting high temperature contact material because DLN provides stability to the contact material. Me-DLN is formed by codepositing metal and DLN. The DLN structure provides an excellent

stabilizing matrix host structure for metals,<sup>11</sup> preventing diffusion and oxidation of the incorporated metal. The resulting Me-DLN structure is significantly more robust while retaining many of the desirable electrical properties of the metal.

The basic amorphous structure of DLN consists of two random interpenetrating networks of carbon and silicon which are stabilized by hydrogen and oxygen, respectively (amorphous C:H, amorphous Si:O). The two networks also mutually stabilize each other by weak chemical forces. Depending on the concentration, the metal is distributed within the Me-DLN as isolated atoms or as a third network.<sup>12</sup> The films are diamond-like in that they contain carbon in a predominantly  $sp^3$  bonding configuration (diamond bonding), but the presence of the silicon network distinguishes them from conventional diamond and diamond-like carbon films.<sup>12</sup> A schematic representation of the DLN structure is depicted in Fig. 1. DLN is deposited by a plasma ion beam line-of-sight vacuum deposition process.<sup>12</sup> A RF bias of 0.5 to 5.0 kV is applied to the target sample during the deposition.<sup>11</sup>

The thermal stability of a metal semiconductor contact depends on the stability of the ambient metal interface, the metal, and the metal semiconductor interface. The thermal stability of Me-DLN, Me-DLN semiconductor interfaces, and alternating stacks of DLN and Me-DLN have been demonstrated by high temperature vacuum anneals. DLN is stable at 1200°C for several hours. Me-DLN remains amorphous (no metal carbide formation) and alternating stacks of DLN and Me-DLN retain abrupt interfaces with no signs of intermixing after a 600°C anneal for 10 h. Me-DLN semiconductor interfaces remain abrupt with no signs of intermixing after a 850°C anneal.<sup>11</sup>

Me-DLN also exhibits excellent thermal stability in air. Platinum-DLN has been shown to be stable in air up to 800°C.<sup>11</sup> Lithium-DLN has also been shown to have only a small amount of surface oxidation when exposed to air while comparable lithium thin films were completely oxidized when exposed to the same conditions.<sup>11</sup> Therefore, Me-DLN should provide an interface which does not oxidize and consequently has a thermally stable interface with an air ambient.

The electrical properties of Me-DLN may be controlled by selecting the metal species and concentration. Many different metals (lithium, silver, copper, aluminum, zinc, magnesium, niobium, tantalum, chromium, molybdenum, tungsten, rhenium, iron, cobalt, and nickel) have been successfully incorporated into DLN. The possible range of metal concentrations (up to 50% while maintaining a Me-DLN structure) allow Me-DLN to have a variable resistivity from  $10^{-4}$  to  $10^{14} \Omega \text{ cm}$ .<sup>13</sup>

The electrical properties of a Me-DLN SiC contact should depend on the metal incorporated into the Me-DLN. SiC has been shown to have a metal semiconductor barrier height which strongly depends on the work function of the metal. Titanium, nickel, and gold contacts to n-type 4H SiC form barrier heights that have a linear dependence on the metal work function

with a slope of 0.7.<sup>14</sup> Therefore, a microelectronics system combining SiC and Me-DLN has potential advantages based on the ability to select the metal incorporated and the capability to withstand high temperatures in air.

**EXPERIMENTAL PROCEDURE**

In this work, tungsten-DLN (W-DLN) has been deposited onto 6H SiC (Si-face) n-type epitaxial layers grown on a heavily doped n-type substrate and p-type epitaxial layers grown on a heavily doped p-type substrate. The SiC material was obtained from Cree Research of Durham, NC. The n-type epitaxial layer doping is  $1.5 \times 10^{16} \text{ cm}^{-3}$  and the layer thickness is 3.0  $\mu\text{m}$ . The p-type epitaxial layer doping is  $1.4 \times 10^{16} \text{ cm}^{-3}$  and the layer thickness is 5.0  $\mu\text{m}$ . Approximately 2000Å of W-DLN (30% to 40% tungsten) was deposited onto the SiC samples through a shadow mask with circular openings of 250  $\mu\text{m}$  in diameter. The W-DLN was deposited by Advanced Refractory Technologies, Inc. Prior to W-DLN deposition, the SiC samples were degreased, etched in hydrofluoric acid (HF), rinsed in deionized (DI) water, blown dry in  $\text{N}_2$ , and in situ plasma cleaned. After W-DLN deposition, a shadow mask fringing effect was observed making the effective device diameter approximately 340  $\mu\text{m}$ . After W-DLN deposition, unannealed large area backside contacts were fabricated. The basic device structure is shown in Fig. 2.

I-V measurements of the n-type and p-type contacts were completed by directly probing the individual contacts and measuring the I-V characteristics on a HP 4145 parameter analyzer. The C-V measurements of the n-type and p-type contacts were also completed by directly probing the individual W-DLN contacts and measuring the C-V characteristics on a HP 4275 LCR meter. All measurements were per-

formed at room temperature.

**RESULTS**

The forward bias I-V characteristics for the n-type and p-type contacts are plotted in Fig. 3. The I-V extracted effective  $\phi_{\text{Bn}}$  is 0.7eV with an ideality factor of 1.2 and the I-V extracted effective  $\phi_{\text{Bp}}$  is 1.8 eV with an ideality factor of 1.7. A I-V extracted  $\phi_{\text{Bn}}$  of 0.79eV with an ideality factor of 1.08 and an I-V extracted  $\phi_{\text{Bp}}$  of 1.57 eV with an ideality factor of 1.20 have been reported for tungsten SiC Schottky contacts.<sup>15</sup> Similar results have been reported for W-DLN Schottky contacts on n-type GaAs<sup>11</sup> with an I-V extracted  $\phi_{\text{Bn}}$  of 0.82 to 0.86 eV and an ideality factor of 1.2 to 1.5. The reverse bias I-V characteristics for the n-type and p-type contacts are shown in Fig. 4. The n-type contacts

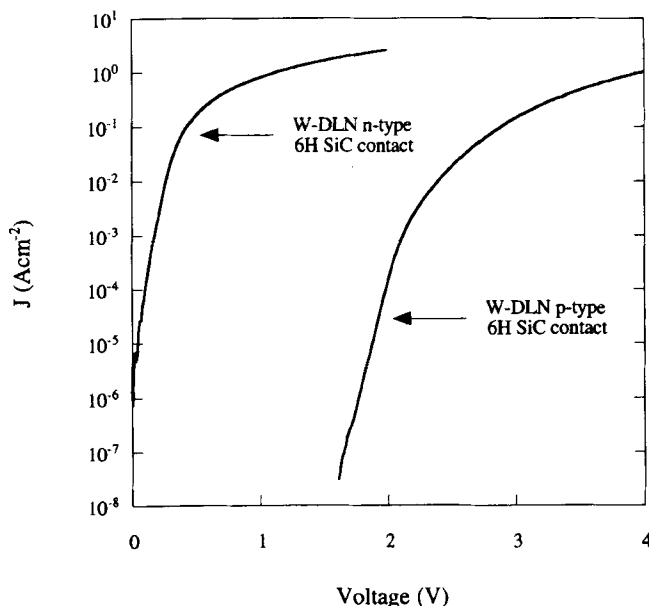


Fig. 3. Forward bias characteristics of W-DLN SiC (Si-face) n-type and p-type Schottky contacts.

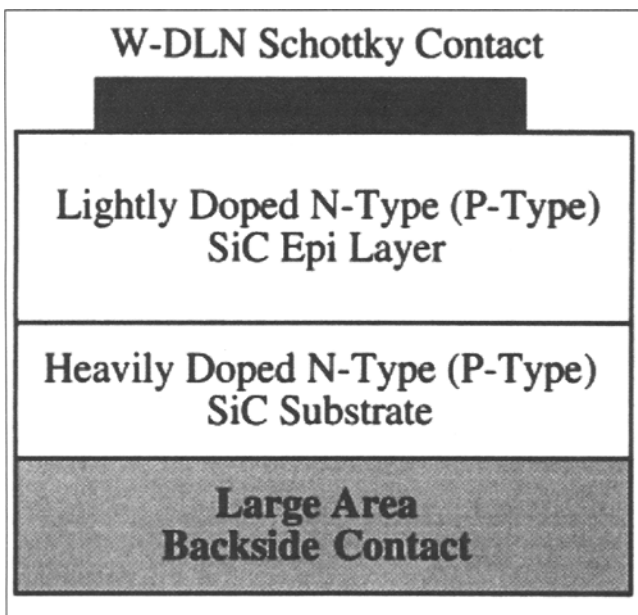


Fig. 2. Device structure of W-DLN Schottky contacts to n-type and p-type 6H SiC.

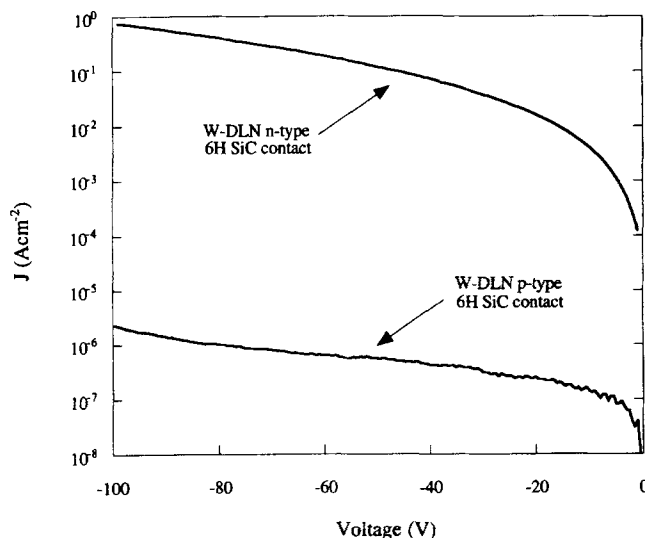


Fig. 4. Reverse bias characteristics of W-DLN SiC (Si-face) n-type and p-type Schottky contacts.

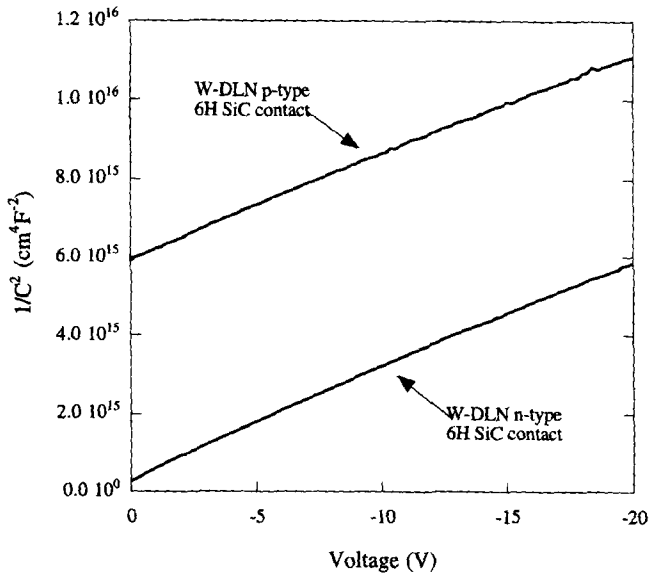


Fig. 5.  $1/C^2$ -V plot of W-DLN SiC (Si-face) n-type and p-type Schottky contacts.

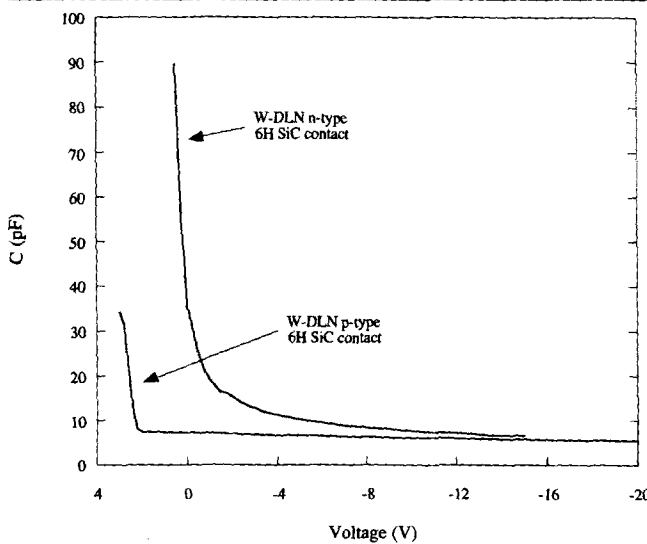


Fig. 6. C-V plot of W-DLN SiC (Si-face) n-type and p-type Schottky contacts.

have a reverse leakage current density of  $4.1 \times 10^{-3} \text{ Acm}^{-2}$  at  $-10 \text{ V}$  and the p-type contacts have a reverse leakage current density of  $1.4 \times 10^{-7} \text{ Acm}^{-2}$  at  $-10 \text{ V}$ .

The  $1/C^2$ -V plots for the n-type and p-type contacts are given in Fig. 5. The n-type contact has a C-V extracted  $V_{bi}$  of 1 V or a  $\phi_{Bn}$  of 1.2 eV. A C-V extracted  $V_{bi}$  and  $\phi_{Bp}$  were not calculated for the p-type contact since the  $1/C^2$ -V curve shows an obvious offset in capacitance. A  $\phi_{Bp}$  of 2.22 eV with no capacitance offset has been reported for tungsten SiC Schottky contacts.<sup>15</sup> The C-V plots for the n-type and p-type contacts are given in Fig. 6. A summary of the W-DLN and reported tungsten I-V and C-V results are given in Table II.

## DISCUSSION

The as-deposited n-type and p-type contacts are rectifying and the electrical characteristics correlate

**Table II. Measured Values for W-DLN SiC (Si-Face) Schottky Contacts and Reported Values for Tungsten SiC Schottky Contacts<sup>15</sup>**

Schottky Type	IV $\phi_B$ (eV)	n	CV $\phi_B$ (eV)
W-DLN n-type	0.7 (effective)	1.2	1.2
W n-type <sup>15</sup>	0.79	1.08	—
W-DLN p-type	1.8 (effective)	1.7	—
W p-type <sup>15</sup>	1.57	1.20	2.22

well with previously reported tungsten SiC Schottky contact results. This suggests that the electrical characteristics are dominated by the properties of the tungsten SiC interface. The large ideality factor, barrier height deviations, non-ideal leakage current, and shift in the p-type C-V may be due to deposition interface damage and nonuniform contact material at the semiconductor interface. Because the target semiconductor was in-situ plasma cleaned before deposition and biased during deposition, fast charged particle interface damage is likely. Deposition of W-DLN onto silicon, germanium, and GaAs has been shown to cause interface damage in the form of dislocation loops. Silicon dislocation loops to a depth of 10 to 15 nm and germanium and GaAs dislocation loops to a depth of 30 to 50 nm have been observed.<sup>11</sup>

In addition, W-DLN will likely form a nonuniform contact to SiC. If W-DLN deposits stoichiometrically onto the semiconductor surface, it will form a nanoscale nonuniform interface where some regions have tungsten in intimate contact with the semiconductor while other regions have either C:H or Si:O in intimate contact with the semiconductor. It has been shown that the I-V measured barrier height will be dominated by the low barrier height interface regions.<sup>16</sup> In addition, the ideality factor will depend on the absolute and relative sizes of the regions.<sup>16</sup> The large ideality factor might also be attributed to an interface damage recombination mechanism or a voltage dependent variation in the barrier height.

The reverse leakage current for the n-type contact is significantly larger than the reverse leakage current for the p-type contact which is consistent with the larger I-V measured effective barrier height of the p-type contact. However, the reverse leakage currents for both the n-type and p-type contacts are larger than the respective barrier heights would theoretically predict. The reverse leakage currents show a stronger voltage dependence than predicted by thermionic emission,<sup>17</sup> image-force barrier height lowering,<sup>17</sup> and thermionic field emission.<sup>18</sup> In addition, neither contact is near the parallel plane breakdown voltage nor is the depletion region punched through the epitaxial layer to the substrate at 100 V reverse bias.

Therefore, the higher than expected reverse leakage currents for both the n-type and the p-type contacts is likely due to a voltage dependent barrier height mechanism and multiplication effects. At 100

V reverse bias, the maximum parallel plane electric field is about  $7.5 \times 10^5$  V/cm. However, without edge termination, field enhancement at the edges of the circular devices can be greater by a factor of 2 or more, which may lead to carrier multiplication effects thereby increasing the reverse leakage current.

The n-type contact  $1/C^2$ -V and C-V plots are normal, but the p-type  $1/C^2$ -V plot is shifted in the direction of a larger than expected  $1/C^2$  value or a smaller than expected capacitance. This shift might be accounted for by the presence of a positive charge near the interface (perhaps from deposition interface damage) which effectively makes the depletion region width larger for a given applied voltage. This increase in the depletion width would correspond to a decrease in the capacitance. The p-type contact C-V curve shows the offset in capacitance that is shown in the  $1/C^2$  curve. The C-V curve also shows that as the contact is strongly forward biased, the capacitance begins to increase significantly, perhaps by the neutralization of a net positive charge near the interface.

It may be possible to prevent deposition interface damage during Me-DLN deposition by either changing the bias of the target semiconductor or by employing a different deposition method. A special method of DLN formation by reflected-flow has been cited as a way to prevent the bombardment of the semiconductor surface by fast charged particles during Me-DLN growth.<sup>11</sup> Solving the problem of deposition interface damage may allow the formation of nearly ideal metal semiconductor contacts with Me-DLN.

### CONCLUSION

The I-V and C-V characteristics of the as-deposited W-DLN Schottky contacts suggest that the electrical properties of the interface are controlled by the properties of the tungsten SiC interface. Therefore, the selection of metal incorporated into a Me-DLN SiC contact should strongly influence the electrical properties of the contact. Me-DLN has previously been shown to provide a protective host matrix which prevents metals from oxidizing, reacting, and diffusing. Hence, it may be possible to fabricate nearly ideal high temperature contacts with defined electrical properties by incorporating a specific metal into Me-

DLN. Based on these measurements, W-DLN and Me-DLN SiC contacts are a potential enabling technology for high temperature rectifying and ohmic contacts.

### ACKNOWLEDGMENT

We would like to thank the NSF Engineering Research Center for Collaborative Manufacturing for their support of this research.

### REFERENCES

1. W. Xie, Y. Wang, M.R. Melloch, J.A. Cooper, Jr., G.M. Johnson, L.A. Lipkin, J.W. Palmour and C.H. Carter, Jr., *Silicon Carbide and Related Materials 1995, Proc. Sixth Intl. Conf.*, (1995), p. 785.
2. S.T. Sheppard, M.R. Melloch and J.A. Cooper Jr., *IEEE Electron Dev. Lett.* 17 (1), 4 (1996).
3. D.B. Slater, Jr., G.M. Johnson, L.A. Lipkin, A.V. Suvorov and J.W. Palmour, *Third Intl. High Temperature Electronics Conf. (HiTEC)*, (1996).
4. N. Ramungul, T.P. Chow, M. Ghezzi, J. Kretschmer and W. Hennessy, *IEEE Device Research Conf.*, (1996).
5. R.C. Clarke, A.K. Agarwal, R.R. Siergiej, C.D. Brandt and A.W. Morse, *IEEE Device Research Conf.*, (1996).
6. J.W. Palmour, R. Singh, L.A. Lipkin and D.G. Waltz, *Third International High Temperature Electronics Conf. (HiTEC)*, (1996).
7. J.N. Shenoy, M.R. Melloch and J.A. Cooper, Jr., *IEEE Device Research Conf.*, (1996).
8. O. Kordina, J.P. Bergman, A. Henry, E. Janzén, S. Savage, J. Andre, L.P. Ramberg, U. Lindefelt, W. Hermansson and K. Bergman, *Appl. Phys. Lett.* 67, 1561 (1995).
9. A. Itoh, T. Kimoto and H. Matsunami, *IEEE Electron Dev. Lett.* 17 (3), 139 (1996).
10. P.G. Neudeck and D.J. Larkin, *1994 NASA Lewis Research & Technology Report*.
11. V.F. Dorfman, A. Bozhko, B.N. Pypkin, R.T. Borra, A.R. Srivatsa, H. Zhang, T.A. Skotheim, I. Khan, D. Rodichev and G. Kirpilenko, *Thin Solid Films* 212, 274 (1992).
12. D.J. Bray, A. Goel and M.T. Spohn, *Advanced Materials and Processes* December, 31 (1994).
13. F.H. Pollak, personal communication.
14. A. Itoh, O. Takemura, T. Kimoto and H. Matsunami, *Silicon Carbide and Related Materials 1995, Pro. Sixth Intl. Conf.* (1995), p. 685.
15. N. Lundberg, P. Tågström, U. Jansson and M. Östling, *Silicon Carbide and Related Materials 1995, Proc. Sixth Intl. Conf.*, (1995), p. 677.
16. J.L. Freeouf, T.N. Jackson, S.E. Laux and J.M. Woodall, *J. Vac. Sci. Technol.* 21 (2), 570 (1982).
17. S.M. Sze, *Physics of Semiconductor Devices*, (New York: John Wiley & Sons).
18. J. Crofton, private communication.